INTERNATIONAL JOURNAL OF CIRCUITS, SYSTEMS AND SIGNAL PROCESSING
DOI: 10.46300/9106.2020.14.22 Volume 14, 2020

# Model for $1/f$ noise in graphene and in more common semiconductors

Paolo Marconcini

*Abstract*—Measurements performed on several graphene samples have shown the presence of a minimum of the flicker noise power spectral density near the charge neutrality point. This behavior is anomalous with respect to what is observed in more usual semiconductors. Here, we report our explanation for this difference. We simulate the $1/f$ noise behavior of devices made of graphene and of more common semiconductors, through a model based on the validity of the mass-action law and on the conservation of the charge neutrality. We conclude that the minimum of the flicker noise at the charge neutrality point can be observed only in very clean samples of materials with similar mobilities for electrons and holes.

*Keywords*—Flicker noise, graphene, silicon, germanium, gallium arsenide, indium arsenide.

## I. Introduction

GRAPHENE is a two-dimensional material made up of one or a few layers of carbon atoms arranged in a hexagonal lattice; in particular, monolayer graphene consists of a single layer of carbon atoms, while bilayer graphene of two coupled layers. Graphene presents quite particular and interesting properties, which have attracted a large interest from the academic and industrial community [1]–[16].

Quite recently, an uncommon flicker noise behavior has been experimentally observed in several graphene samples. Flicker (or $1/f$) noise is one of the main types of electronic noise measured in electronic devices, characterized by a power spectral density inversely proportional to the frequency $f$. Flicker noise originates from the presence of impurities (traps) located inside or near the conducting channel of the considered device; these impurities, randomly trapping and detrapping electrons from and into the channel give rise to the random current fluctuations which represent the noise.

In common semiconductors, flicker noise power spectral density $S_I$ approximately follows the empirical Hooge formula [17], according to which it should be inversely proportional to the number of free charge carriers.

On the contrary, measures of flicker noise in graphene have shown a more complex scenario [18]–[24]. While in most graphene samples a $\Lambda$-shaped behavior has been observed as a function of charge density or of Fermi energy, in several bilayer and suspended monolayer graphene samples an M-shaped behavior has been found, with a minimum at the charge neutrality point, in contrast with what is predicted by the Hooge formula. In the following, we will describe our model [25], [26], which explains the experimentally observed flicker noise behavior on the basis of the conservation of the mass-action law and of the electroneutrality in the device. Using this model, we will compare the behavior of graphene and of more common semiconductors, and we will conclude that a minimum in the flicker noise power spectral density is possible only if electrons and holes have approximately the same mobility, as in the case of graphene, and if potential disorder in the device is very low.

This work was partially supported by the Italian Ministry of Education and Research (MIUR) in the framework of the CrossLab project (Departments of Excellence).

Paolo Marconcini is with the Dipartimento di Ingegneria dell'Informazione, Università di Pisa, Via Girolamo Caruso 16, 56122 Pisa, Italy

## II. Model

Let us first consider a two-dimensional device, with length $L$ in the transport direction $x$ and width $W$ in the transverse direction $y$ (and thus with area $A = LW$). The macroscopic current at the terminals of the considered device can be related to the microscopic phenomena taking place inside the device through the Ramo-Shockley-Pellegrini theorem [27]–[29]. In detail, the current $i$ at the terminals of the device can be expressed as:

$$i = \frac{1}{L}\int_A q(\mu_n n + \mu_p p)E\,dx\,dy\,, \tag{1}$$

where $q$ is the modulus of the elementary charge, $E$ is the modulus of the electric field (oriented in the $x$ direction), $n$ and $p$ are the electron and hole surface densities, and $\mu_n$ and $\mu_p$ are the electron and hole mobilities, respectively. Here, we have related the current at the terminals to the drift current inside the device weighting in each point of the device the contribution of the drift current through a uniform function $(1/L)\hat{x}$. In the case of three-dimensional devices, this model can be generalized substituting the superficial integral with a volumetric integral and redefining $n$ and $p$ as volumetric densities.

Assuming the main effect of the trapping/detrapping phenomena to be a variation of electron and hole densities, and dividing the current fluctuations $\Delta i$ by the mean drift current $I = q(\mu_n n + \mu_p p)EW$, we obtain

$$\frac{\Delta i}{I} = \frac{\int_A q(\mu_n \Delta n + \mu_p \Delta p)E\,dx\,dy}{LW q(\mu_n n + \mu_p p)E} \approx \frac{\mu_n \Delta N + \mu_p \Delta P}{\mu_n N + \mu_p P}, \tag{2}$$

where $N = \int_A n\,dx\,dy$ and $P = \int_A p\,dx\,dy$.

Let us refer the variations to the condition in which the trap is empty. Following this choice, if the trap is empty $\Delta N$ and $\Delta P$ are zero. Instead, the values of $\Delta N$ and $\Delta P$ when an electron is trapped can be found enforcing the conservation of the mass-action law and of the charge neutrality of the device, i.e. solving the system

$$\begin{cases} N\Delta P + P\Delta N = 0 \\ \Delta P - \Delta N = 1 \end{cases} \tag{3}$$

(the first equation is obtained differentiating the mass-action law, the second one enforcing a zero total charge variation). Solving this system, we obtain $\Delta N = -N/(P+N)$ and $\Delta P = P/(P+N)$. This means that the charge of the electron trapped in the impurity is mainly electrostatically screened by a local reduction of mobile electrons for the energies for which the electrons are the dominating carriers, by a local increase of mobile holes for the energies for which the holes are the dominating carriers, and by a combined action of the two effects for intermediate energies. Substituting these expressions inside Eq. (2), we obtain that:

$$\frac{\Delta i}{I} = \frac{1}{\mu_n N + \mu_p P} \frac{\mu_p P - \mu_n N}{P+N} \chi \tag{4}$$

(where $\chi$ is a random telegraph process which is equal to 0 when the trap is empty and to 1 when the trap is full). Therefore, its power spectral density $S_I$ is:

$$\frac{S_I}{I^2} = \left( \frac{1}{\mu_n N + \mu_p P} \frac{\mu_p P - \mu_n N}{P+N} \right)^2 S_\chi \,, \tag{5}$$

where (neglecting the contribution of the mean value) $S_\chi(f)$ is a Lorentzian function.

Combining the contribution of several traps, assumed reciprocally independent and with properly distributed time constants, we obtain [30]

$$\frac{S_I}{I^2} = \xi \left( \frac{1}{\mu_n N + \mu_p P} \frac{\mu_p P - \mu_n N}{P+N} \right)^2 \frac{1}{f^\gamma} \tag{6}$$

with $\gamma \approx 1$ (i.e., the characteristic $1/f$ dependence of flicker noise).

The spectrum vanishes when $\mu_p P - \mu_n N = 0$. In the particular case in which $\mu_n = \mu_p$, this represents the charge neutrality point and the spectrum is symmetric with respect to it. Otherwise, the spectrum is asymmetric, with a larger value where the carriers with higher mobility dominate.

Also the presence of potential disorder, deriving from the electrostatic effect of randomly located charged impurities, has a large impact on the noise spectrum. Indeed, $N$ and $P$ depend on the position of the Fermi energy with respect to the local value of the potential. The random spatial distribution of the potential is included in the calculation by averaging the spectrum over a Gaussian distribution of energies around the average value $E_F$:

$$\frac{\langle S_I \rangle}{I^2} = \frac{\xi}{f^\gamma} \int_{-\infty}^{+\infty} \left( \frac{1}{\mu_n N(\varepsilon) + \mu_p P(\varepsilon)} \cdot \right.$$
$$\left. \cdot \frac{\mu_p P(\varepsilon) - \mu_n N(\varepsilon)}{P(\varepsilon) + N(\varepsilon)} \right)^2 \frac{1}{\sqrt{2\pi\sigma^2}} e^{-\frac{(\varepsilon - E_F)^2}{2\sigma^2}} \, d\varepsilon \,. \tag{7}$$

The standard deviation $\sigma$ represents a measure of the strength of the potential disorder, and thus depends on the quantity and distribution of the charged impurities, and on the screening efficiency of the material.

## III. Results

We have first simulated the flicker noise behavior of two-dimensional devices based on monolayer graphene and on bilayer graphene with Bernal stacking. In graphene, the electron and hole mobilities coincide, and thus in the relations of the previous section we can consider $\mu_n = \mu_p = \mu$.

The carrier concentrations are computed through an energy integration of the occupied states in the conduction band, and of the empty states in the valence band, respectively [31]:

$$n = \int_0^\infty DOS(E) f(E - E_F) \, dE \,, \tag{8}$$

$$p = \int_{-\infty}^0 DOS(E)(1 - f(E - E_F)) \, dE \,, \tag{9}$$

Here, $f$ is the Fermi-Dirac occupation function, while $DOS$ is the density of states, which is obtained from the dispersion relations of graphene. These last relations are approximately symmetric with respect to the Dirac points (i.e. the degeneration points between the valence and the conduction band, where we consider $E = 0$).

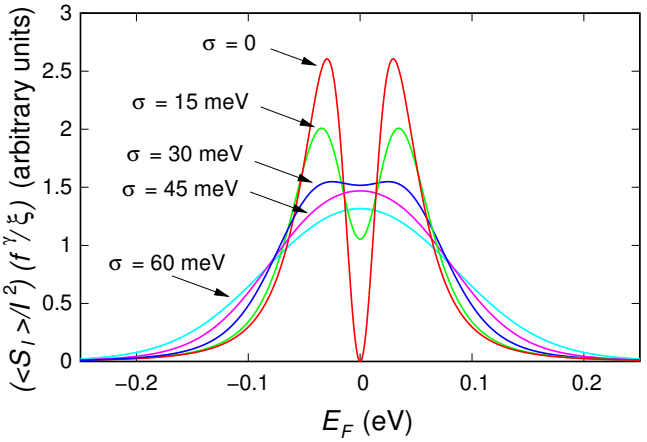


Fig. 1. Normalized spectrum $(\langle S_I \rangle / I^2)(f^\gamma/\xi)$ as a function of the Fermi energy $E_F$, obtained for monolayer graphene at 300 K. The curve for $\sigma = 0$ has been obtained in the absence of potential disorder, while the other curves show the effect of a potential disorder with a Gaussian distribution with $\sigma =$ 15, 30, 45, and 60 meV.

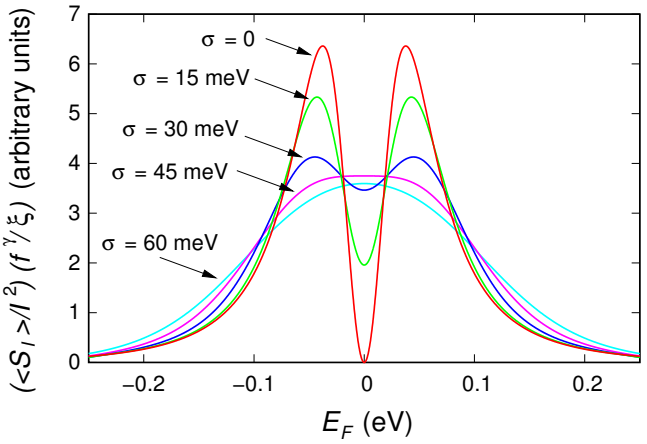


Fig. 2. Normalized spectrum $(\langle S_I \rangle / I^2)(f^\gamma/\xi)$ as a function of the Fermi energy $E_F$, obtained for bilayer graphene at 300 K. The curve for $\sigma = 0$ has been obtained in the absence of potential disorder, while the other curves show the effect of a potential disorder with a Gaussian distribution with $\sigma =$ 15, 30, 45, and 60 meV.

In Figs. 1 and 2, the curves with $\sigma = 0$ represent the behavior of the flicker noise power spectral density as a function of the Fermi energy for monolayer and bilayer graphene, respectively, at 300 K without including the effect of potential disorder. As we expected, the spectrum is symmetric with respect to the charge neutrality point, i.e. to the Dirac points, where it vanishes. Indeed, in this point (where $q(P-N)=0$) $\Delta N = -\Delta P$ and thus the current fluctuations vanish (see Eqs. (2) and (5).

In Figs. 1 and 2 we report also the flicker noise power spectral density as a function of the Fermi energy for monolayer and bilayer graphene, respectively, at 300 K when the effect of potential disorder is included in the calculation. Three different nonzero values for the standard deviation $\sigma$ are considered: $\sigma = 15$, 30, 45, and 60 meV. We notice that increasing the potential disorder (i.e. increasing $\sigma$), we have a smoothing of the spectrum behavior, with a progressive reduction, and finally disappearance, of the minimum. In particular, due to the different dispersion relations, bilayer graphene is able to electrostatically screen the effect of charged impurities better than monolayer graphene. Therefore, for a similar impurity distribution, smaller values of $\sigma$ should be considered for bilayer graphene with respect to monolayer graphene. This would explain why experiments in bilayer graphene often show a minimum of the spectrum at the charge neutrality point, while in monolayer graphene such a minimum is rarely observed, apart in the case of suspended graphene (where the electrostatic effect of the charged impurities is small).

Then, we have analyzed the case of three-dimensional devices fabricated in more common semiconductors, which present a different mobility for electrons and holes (here, we report results for silicon, germanium, gallium arsenide, and indium arsenide). In this case, we have adopted a semiclassical modelization for the carrier concentrations:

$$n = N_C\, e^{-\frac{E_C - E_F}{k_B T}}\ , \quad p = N_V\, e^{-\frac{E_F - E_V}{k_B T}}\ , \qquad (10)$$

where $N_C$ and $N_V$ are the effective densities of states in the conduction and valence bands, respectively, $E_C$ and $E_V$ the conduction and valence band edges, $k_B$ the Boltzmann constant, and $T$ the absolute temperature.

The parameters used for the four considered materials are reported in Tables I and II [32].

In Figs. 3, 4, 5, and 6, the curves with $\sigma = 0$ represent the flicker noise power spectral density behavior as a function of the Fermi energy at 300 K obtained for silicon, germanium, gallium arsenide, and indium arsenide, respectively, in the absence of potential disorder. The spectrum vanishes for the energy value for which $\mu_p P - \mu_n N = 0$ (that in this case does not correspond to the charge neutrality point) and is not symmetric with respect to this point, because $\mu_n$ and $\mu_p$ differ. This asymmetry is more visible in the cases of gallium arsenide and indium arsenide, where the difference between the electron and hole mobilities is larger. Due to the asymmetry, in this case the presence of the minimum (where the spectrum vanishes) is much less prominent than in graphene: in gallium arsenide and in indium arsenide, in particular, it can hardly be distinguished from the region for smaller Fermi energies, where the flicker noise power spectrum density is lower.

The other curves of Figs. 3, 4, 5, and 6 show the flicker noise power spectral density behavior as a function of the Fermi energy at 300 K obtained for silicon, germanium, gallium arsenide, and indium arsenide, respectively, when the effect of potential disorder is included in the simulations (with $\sigma = 15$, 30, 45, and 60 meV). It clearly appears that, in these materials, the minimum of the spectrum does not survive in the presence of even a small degree of potential disorder, as experimentally observed [33].

TABLE I
VALUES OF THE EFFECTIVE DENSITIES OF STATES, OF THE ENERGY GAP, AND OF THE MOBILITIES USED FOR SILICON AND GERMANIUM.

| | Si | Ge |
|---|---|---|
| $N_C$ (cm$^{-3}$) | $2.82 \times 10^{19}$ | $1.0 \times 10^{19}$ |
| $N_V$ (cm$^{-3}$) | $1.04 \times 10^{19}$ | $5.0 \times 10^{18}$ |
| $E_G$ (eV) | 1.12 | 0.66 |
| $\mu_n$ (cm$^2$/(V s)) | 1400 | 3900 |
| $\mu_p$ (cm$^2$/(V s)) | 450 | 1900 |

TABLE II
VALUES OF THE EFFECTIVE DENSITIES OF STATES, OF THE ENERGY GAP, AND OF THE MOBILITIES USED FOR GALLIUM ARSENIDE AND INDIUM ARSENIDE.

| | GaAs | InAs |
|---|---|---|
| $N_C$ (cm$^{-3}$) | $4.7 \times 10^{17}$ | $8.7 \times 10^{16}$ |
| $N_V$ (cm$^{-3}$) | $7.0 \times 10^{18}$ | $6.6 \times 10^{18}$ |
| $E_G$ (eV) | 1.42 | 0.35 |
| $\mu_n$ (cm$^2$/(V s)) | 8500 | 40000 |
| $\mu_p$ (cm$^2$/(V s)) | 400 | 500 |

## IV. CONCLUSION

Comparing the flicker noise behavior of graphene and of more common semiconductors, such as silicon, germanium, gallium arsenide, and indium arsenide, we conclude that the presence of a minimum of the flicker noise power spectral density around the charge neutrality point should be observable only in devices made up by materials with approximately identical electron and hole mobilities, like graphene, and with a very low level of potential disorder. Otherwise, we do not expect such a minimum to appear. This would explain the difference between the $1/f$ noise behavior measured in many graphene samples and that of more ordinary semiconductors.

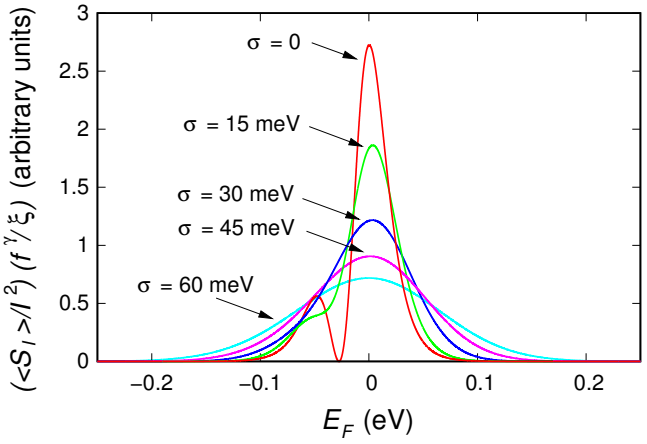


Fig. 3. Normalized spectrum $(\langle S_I \rangle / I^2)(f^\gamma/\xi)$ as a function of the Fermi energy $E_F$, obtained for silicon at 300 K. The curve for $\sigma = 0$ has been obtained in the absence of potential disorder, while the other curves show the effect of a potential disorder with a Gaussian distribution with $\sigma = 15$, 30, 45, and 60 meV.

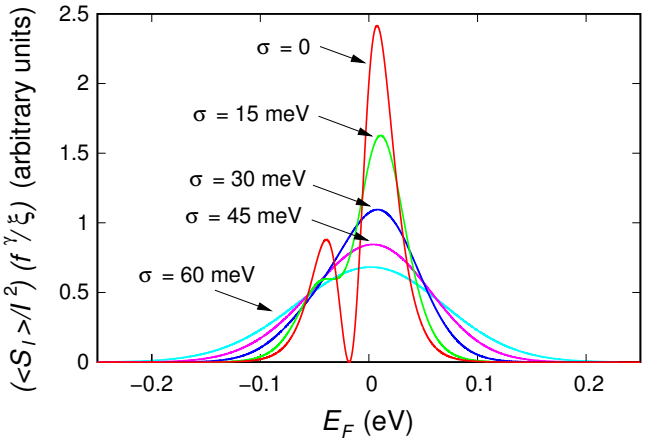


Fig. 4. Normalized spectrum $(\langle S_I \rangle / I^2)(f^\gamma/\xi)$ as a function of the Fermi energy $E_F$, obtained for germanium at 300 K. The curve for $\sigma = 0$ has been obtained in the absence of potential disorder, while the other curves show the effect of a potential disorder with a Gaussian distribution with $\sigma = 15$, 30, 45, and 60 meV.

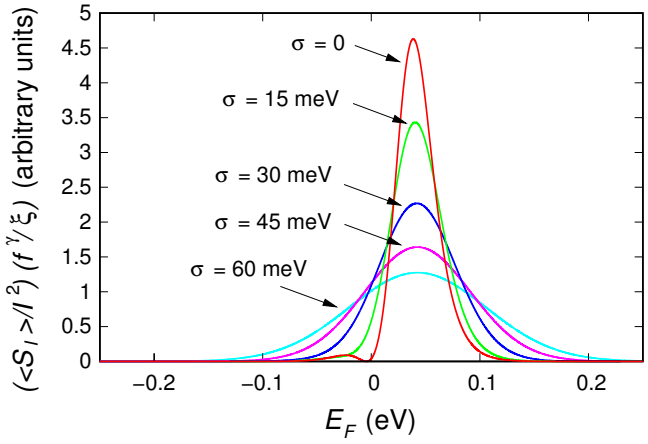


Fig. 5. Normalized spectrum $(\langle S_I \rangle / I^2)(f^\gamma/\xi)$ as a function of the Fermi energy $E_F$, obtained for gallium arsenide at 300 K. The curve for $\sigma = 0$ has been obtained in the absence of potential disorder, while the other curves show the effect of a potential disorder with a Gaussian distribution with $\sigma = 15$, 30, 45, and 60 meV.

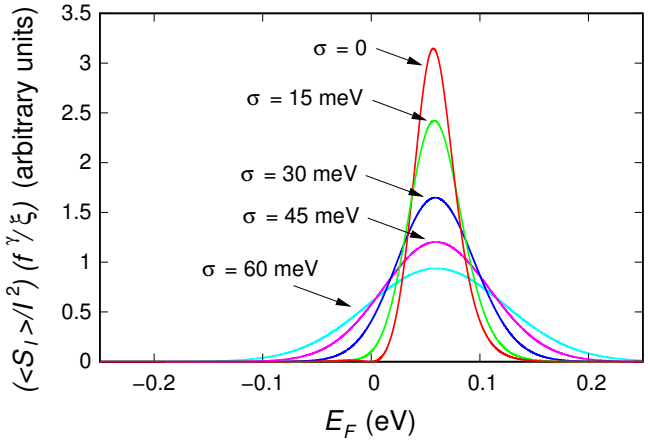


Fig. 6. Normalized spectrum $(\langle S_I \rangle / I^2)(f^\gamma/\xi)$ as a function of the Fermi energy $E_F$, obtained for indium arsenide at 300 K. The curve for $\sigma = 0$ has been obtained in the absence of potential disorder, while the other curves show the effect of a potential disorder with a Gaussian distribution with $\sigma = 15$, 30, 45, and 60 meV.

## ACKNOWLEDGMENT

This work was partially supported by the Italian Ministry of Education and Research (MIUR) in the framework of the CrossLab project (Departments of Excellence).

## REFERENCES

[1] K. S. Novoselov, A. K. Geim, S. V. Morozov, D. Jiang, M. I. Katsnelson, I. V. Grigorieva, S. V. Dubonos, and A. A. Firsov, "Two-dimensional gas of massless Dirac fermions in graphene," *Nature*, vol. 438, pp. 197–200, 2005, DOI: 10.1038/nature04233.

[2] A. K. Geim and K. S. Novoselov, "The rise of graphene," *Nat. Mater.*, vol. 6, pp. 183–191, 2007, DOI: 10.1038/nmat1849.

[3] A. H. Castro Neto, F. Guinea, N. M. R. Peres, K. S. Novoselov and A. K. Geim, "The electronic properties of graphene," *Rev. Mod. Phys.*, vol. 81, pp. 109–162, 2009, DOI: 10.1103/RevModPhys.81.109.

[4] P. Marconcini, M. Macucci, "The k·p method and its application to graphene, carbon nanotubes and graphene nanoribbons: the Dirac equation," *Riv. Nuovo Cimento*, vol. 34, pp. 489–584, 2011, DOI: 10.1393/ncr/i2011-10068-1.

[5] M. I. Katsnelson, K. S. Novoselov, and A. K. Geim, "Chiral tunnelling and the Klein paradox in graphene," *Nat. Phys.*, vol. 2, pp. 620–625, 2006, DOI: 10.1038/nphys384.

[6] E. D. Herbschleb, R. K. Puddy, P. Marconcini, J. P. Griffiths, G. A. C. Jones, M. Macucci, C. G. Smith, and M. R. Connolly, "Direct imaging of coherent quantum transport in graphene p-n-p junctions," *Phys. Rev. B*, vol. 92, p. 125414, 2015, DOI: 10.1103/PhysRevB.92.125414.

[7] P. Marconcini and M. Macucci, "Geometry-dependent conductance and noise behavior of a graphene ribbon with a series of randomly spaced potential barriers," *J. Appl. Phys.*, vol. 125, p. 244302, 2019, DOI: 10.1063/1.5092512.

[8] J. Tworzydło, B. Trauzettel, M. Titov, A. Rycerz, and C. W. J. Beenakker, "Sub-Poissonian shot noise in graphene," *Phys. Rev. Lett.*, vol. 96, p. 246802, 2006, DOI: 10.1103/PhysRevLett.96.246802.

[9] M. Fagotti, C. Bonati, D. Logoteta, P. Marconcini, and M. Macucci, "Armchair graphene nanoribbons: $\mathcal{PT}$-symmetry breaking and exceptional points without dissipation," *Phys. Rev. B*, vol. 83, p. 241406(R), 2011, DOI: 10.1103/PhysRevB.83.241406.

[10] K. S. Novoselov, E. McCann, S. V. Morozov, V. I. Fal'ko, M. I. Katsnelson, U. Zeitler, D. Jiang, F. Schedin, and A. K. Geim, "Unconventional quantum Hall effect and Berry's phase of $2\pi$ in bilayer graphene," *Nat.*

*Phys.*, vol. 2, pp. 177–180, 2006, DOI: 10.1038/nphys245.

[11] M. R. Connolly, R. K. Puddy, D. Logoteta, P. Marconcini, M. Roy, J. P. Griffiths, G. A. C. Jones, P. A. Maksym, M. Macucci, and C. G. Smith, "Unraveling Quantum Hall Breakdown in Bilayer Graphene with Scanning Gate Microscopy," *Nano Lett.*, vol. 12, pp. 5448–5454, 2012, DOI: 10.1021/nl3015395.

[12] V. V. Cheianov, V. Fal'ko, and B. L. Altshuler, "The focusing of electron flow and a Veselago lens in graphene p-n junctions," *Science*, vol. 315, pp. 1252–1255 (2007), DOI: 10.1126/science.1138020.

[13] A. C. Ferrari, F. Bonaccorso, V. Fa'lko, K. S. Novoselov, S. Roche, P. Bøggild, S. Borini, F. H. L. Koppens, V. Palermo, N. Pugno, J. A. Garrido, R. Sordan, A. Bianco, L. Ballerini, M. Prato, E. Lidorikis, J. Kivioja, C. Marinelli, T. Ryhänen, A. Morpurgo, J. N. Coleman, V. Nicolosi, L. Colombo, A. Fert, M. Garcia-Hernandez, A. Bachtold, G. F. Schneider, F. Guinea, C. Dekker, M. Barbone, Z. Sun, C. Galiotis, A. N. Grigorenko, G. Konstantatos, A. Kis, M. Katsnelson, L. Vandersypen, A. Loiseau, V. Morandi, D. Neumaier, E. Treossi, V. Pellegrini, M. Polini, A. Tredicucci, G. M. Williams, B. H. Hong, J.-H. Ahn, J. M. Kim, H. Zirath, B. J. van Wees, H. van der Zant, L. Occhipinti, A. Di Matteo, I. A. Kinloch, T. Seyller, E. Quesnel, X. Feng, K. Teo, N. Rupesinghe, P. Hakonen, S. R. T. Neil, Q. Tannock, T. Löfwander, and J. Kinaret, "Science and technology roadmap for graphene, related two- dimensional crystals, and hybrid systems," *Nanoscale*, vol. 7, pp. 4598–4810, 2015, DOI: 10.1039/C4NR01600A.

[14] P. Marconcini and M. Macucci, "Symmetry-dependent transport behavior of graphene double dots," *J. Appl. Phys.*, vol. 114, p. 163708, 2013, DOI: 10.1063/1.4827382.

[15] P. Marconcini and M. Macucci, "Envelope-function based transport simulation of a graphene ribbon with an antidot lattice," *IEEE Trans. Nanotechnol.*, vol. 16, pp. 534–544, 2017, DOI: 10.1109/TNANO.2016.2645663.

[16] Y. Zhu, H. Ji, H.-M. Cheng, and R. S. Ruoff, "Mass production and industrial applications of graphene materials," *Natl. Sci. Rev.*, vol. 5, pp. 90–101, 2018, DOI: 10.1093/nsr/nwx055.

[17] F. N. Hooge, "$1/f$ noise is no surface effect," *Phys. Lett. A*, vol. 29, pp. 139–140, 1969, DOI: 10.1016/0375-9601(69)90076-0.

[18] A. A. Balandin, "Low-frequency $1/f$ noise in graphene devices," *Nat. Nanotechnol.*, vol. 8, pp. 549–555, 2013, DOI: 10.1038/nnano.2013.144.

[19] Y. Lin and P. Avouris, "Strong suppression of electrical noise in bilayer graphene nanodevices," *Nano Lett.*, vol. 8, pp. 2119–2125, 2008, DOI: 10.1021/nl080241l.

[20] A. N. Pal and A. Ghosh, "Ultralow noise field-effect transistor from multilayer graphene," *Appl. Phys. Lett.*, vol. 95, p. 082105, 2009, DOI: 10.1063/1.3206658.

[21] G. Xu, C. M. Jr. Torres, Y. Zhang, F. Liu, E. B. Song, M. Wang, Y. Zhou, C. Zeng, and K. L. Wang, "Effect of Spatial Charge Inhomogeneity on $1/f$ Noise Behavior in Graphene," *Nano Lett.*, vol. 10, pp. 3312–3317, 2010, DOI: 10.1021/nl100985z.

[22] I. Heller, S. Chatoor, J. Maennik, M. A. G. Zevenbergen, J. B. Oostinga, A. F. Morpurgo, C. Dekker, and S. G. Lemay, "Charge noise in graphene transistors," *Nano Lett.*, vol. 10, pp. 1563–1567, 2010, DOI: 10.1021/nl903665g.

[23] A. N. Pal, S. Ghatak, V. Kochat, E. S. Sneha, A. Sampathkumar, A. Raghavan, and A. Ghosh, "Microscopic mechanism of $1/f$ noise in graphene: role of energy band dispersion," *ACS Nano*, vol. 5, pp. 2075–2081, 2011, DOI: 10.1021/nn103273n.

[24] Y. Zhang, E. E. Mendez, and X. Du, "Mobility-dependent low frequency noise in Graphene field effect transistors," *ACS Nano*, vol. 5, pp. 8124–8130, 2011, DOI: 10.1021/nn202749z.

[25] M. Macucci and P. Marconcini, "Theoretical comparison between the flicker noise behavior of graphene and of ordinary semiconductors," *J. Sensors*, vol. 2020, p. 2850268, 2020, DOI: 10.1155/2020/2850268.

[26] B. Pellegrini, P. Marconcini, M. Macucci, G. Fiori, and G. Basso, "Carrier density dependence of 1/f noise in graphene explained as a result of the interplay between band-structure and inhomogeneities," *J. Stat. Mech.: Theory Exp.*, vol. 2016, p. 054017, 2016, DOI: 10.1088/1742-5468/2016/05/054017.

[27] S. Ramo, "Currents Induced by Electron Motion," *Proc. IRE.*, vol. 27, pp. 584–585, 1939, DOI: 10.1109/JRPROC.1939.228757.

[28] W. Shockley, "Currents to Conductors Induced by a Moving Point Charge," *J. Appl. Phys.*, vol. 9, pp. 635–636, 1938, DOI: 10.1063/1.1710367.

[29] B. Pellegrini, "Electric charge motion, induced current, energy balance, and noise," *Phys. Rev. B*, vol. 34, pp. 5921–5924, 1986, DOI: 10.1103/PhysRevB.34.5921.

[30] A. L. McWhorter, "$1/f$ noise and germanium surface properties," in *Semiconductor Surface Physics*, R. H. Kingston, Ed., University of Pennsylvania Press, Philadelphia, PA, USA, pp. 207–228, 1957, ISBN: 1258339684.

[31] P. Marconcini and M. Macucci, "Approximate calculation of the potential profile in a graphene-based device," *IET Circ. Device Syst.*, vol. 9, pp. 30–38, 2015, DOI: 10.1049/iet-cds.2014.0003.

[32] M. Levinshtein, S. Rumyantsev, and M. Shur, *Handbook Series on Semiconductor Parameters. Volume 1: Si, Ge, C (Diamond), GaAs, GaP, GaSb, InAs, InP, InSb*. Singapore: World Scientific Publishing, 1996, ISBN: 9810229348.

[33] F. N. Hooge, T. G. M. Kleinpenning, and L. K. J. Vandamme, "Experimental studies on $1/f$ noise," *Rep. Prog. Phys.*, vol. 44, p. 479–532, 1981, DOI: 10.1088/0034-4885/44/5/001.

**Paolo Marconcini** Paolo Marconcini received the Master's (summa cum laude) degree in Electrical Engineering and the Ph.D. degree in Electrical and Computer Engineering from the Università di Pisa, Pisa, Italy, in 2002 and 2006, respectively. From 2006, he has been a Post-Doctoral Researcher and then Tenure-Track Researcher with the Università di Pisa, where he is now Associate Professor. He has authored over 100 papers in international journals and proceedings and has been involved in over ten national and international research projects. His current research interests include the study of nanoelectronic devices based on semiconductor heterostructures, nanowires, carbon nanotubes, graphene and two-dimensional materials, and of electronic systems for transportation.